Dynamic light scattering from an optically trapped microsphere

N. B. Viana, R. T. S. Freire, and O. N. Mesquita
Departamento de Física, ICEX, Universidade Federal de Minas Gerais, Caixa Postal 702, Belo Horizonte, CEP 30123-970, MG, Brazil
(Received 23 October 2001; published 10 April 2002)

Using a single microscope objective lens to optically trap, illuminate, and collect backscattered light of a dielectric microsphere, we measure the temporal-intensity-autocorrelation functions (ACFs), and intensity profiles to obtain the trap stiffness and friction coefficient of the bead. This is an interesting study of an harmonically bound Brownian particle, with nanometer resolution. We extend the work of Bar-Ziv *et al.* [Phys. Rev. Lett. **78**, 154 (1997)] to more general situations allowing for the use of our simpler geometry in other applications. As examples, we present measurements of the parallel Stokes friction coefficient on the trapped bead as a function of its distance from a surface and the entropic force of a single λ-DNA molecule.

DOI: 10.1103/PhysRevE.65.041921 PACS number(s): 87.64.−t, 05.40.−a, 42.25.Fx

I. INTRODUCTION

A single laser beam focused by a high numerical aperture microscope objective can trap particles near its focus. This arrangement is called an optical tweezer [1]. The use of optical tweezers to manipulate small objects has been applied to many problems of biological interest. Typically, forces in the pico-Newton range are obtained. Recently, exact axial and transverse forces exerted by optical tweezers on a dielectric microsphere were calculated [2]. By attaching one end of a single DNA molecule to a polystyrene bead (diameter 1 to 3 μm) and the other end to a microscope slide, one can stretch a DNA molecule by pulling the bead with an optical tweezer. By knowing the tweezer's stiffness and measuring the displacement of the trapped bead in relation to its original equilibrium position we can determine the force applied to stretch the DNA molecule. For a review see Strick *et al.* [3], and references therein. To determine the stiffness of an optical tweezer several methods have been discussed in the literature [4,5]. The trapped bead is a prototype of a Brownian harmonic oscillator. Therefore, the tweezer's stiffness can be obtained from measurements of the Brownian fluctuations of the bead. Quasielastic-dynamic-light scattering (QEDLS) is an excellent tool to probe Brownian fluctuations of small colloidal particles [6]. In the last three decades, QEDLS has been extensively used to study colloidal particle and macromolecule diffusion, Doppler velocimetry in hydrodynamics, chemical reactions, surface phenomena at growing solid-liquid interfaces, as well as phase transitions in liquid crystals and in polymers, among others. In these applications, in the homodine configuration, the sample is illuminated with a single laser beam whose waist is much larger than the typical size of the light scatterers, such that many of them are in the scattering region. The total scattered light that falls on a photodetector is the sum of the light scattered by each individual scatterer. Since they move in relation to each other, the scattered electric fields relative phases change and, due to interference, the total light intensity in the photodetector fluctuates in time as determined by the dynamics of the scatterers. Clearly, if only a single scatterer is within the uniformly illuminated scattering volume, the scattered light intensity on the detector will be constant even if the scatterer moves around. However, if the laser beam waist is smaller than the size of the scatterer, the scattered intensity depends on the position of the scatterer in relation to the beam. Small fluctuations of the scatterer position in relation to the center of the laser beam will result in scattered intensity fluctuations. In our case, an infrared (IR) laser beam traps a polystyrene bead of 2.8 μm diameter, that is illuminated by a He-Ne laser beam with a waist around 0.6 μm. In Fig. 1 we show the schematic drawing of our experimental setup, that will be detailed in Sec. III A.

There will be light intensity fluctuations that are related to the Brownian motion of the trapped bead. From the temporal-intensity autocorrelation function (ACF) one can obtain the trap stiffness. This approach was first demon-

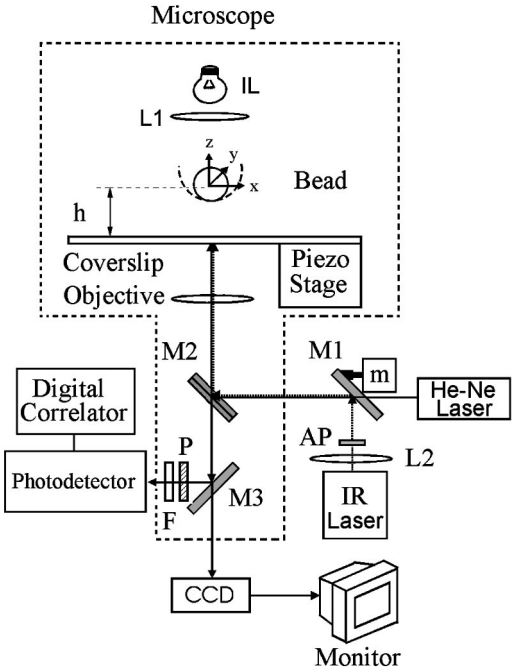

FIG. 1. Experimental setup around the Nikon TE300. *L2* is a microscope 20X objective, AP is an anamorphic prism, *M1* and *M2* are dicroic mirrors for maximizing IR reflections, *m* is a d.c. motor to move the IR beam, *M3* is a movable prism inside the microscope to switch different paths, *P* is a polarizer, *F* is a 632.8 nm line filter, the Photodetector is an EG&G SPCM-0200, and the Digital Correlator is a Brookhaven BI-9000AT.

strated by Bar-Ziv *et al.* [7], and can be applied to more general situations where the light scattering is caused by any quasilocalized scatterer. Bar-Ziv *et al.* coined the name localized dynamic light scattering (LDLS) for this arrangement. In this paper we extend their work to more general situations. Their theoretical derivations and experiments are only applicable if the average position of the scatterer is located at the peak of the scattering function. We extend their derivation allowing other positions for the scatterer in relation to the scattering peak and discuss the advantages of doing so. This generalization allows us to use a simpler collection optics, that may make this technique more attractive and easier to use. We work in a backscattering geometry which is advantageous to use together with optical tweezers, since the same microscope objective is used to optically trap a bead (IR laser), to illuminate it (He-Ne laser), and to collect the backscattered light intensity that falls into a photodetector. From the decay time of the ACF we obtain the trap stiffness if we know the friction on the bead; from its amplitude we obtain the trap stiffness if we know the light scattering profile. Therefore, to fully exploit this technique in this geometry, we have to measure precisely the light scattering profile, which depends on the position of the photodetector and the spheres used. Differences in light scattering from one sphere to another require the measurement of the intensity profile in each experimental run. However, this technique allows us to selectively measure the stiffness along each direction. By simultaneously measuring both relaxation time and amplitude of the fluctuations in the nanometer scale, we present a complete and beautiful illustration of the physics of a harmonically bound Brownian particle. In addition, as applications of this technique, we measure the parallel Stokes friction on a microsphere as a function of its height in relation to a surface and the entropic elasticity of λ-DNA.

II. THEORY

Our scatterer is a rigid polystyrene sphere of 2.8 μm diameter trapped in the anisotropic potential well of an optical tweezer. There are no internal degrees of freedom, consequently the only particle variable is its center of mass position, that is specified in relation to the position of the scattering function profile peak. In Sec. III we will describe how we can do that. We use a Cartesian coordinate system that is specified by taking its origin at the peak of the scattering profile with the z direction along the propagation direction of both IR and He-Ne laser beams. The scattering profile is determined by the position of the particle in relation to the incident He-Ne laser and by the photodetector's position. Examples of such profiles are shown in Figs. 2 and 3.

Figure 2 displays a profile where the He-Ne laser is aligned with the photodetector. The profile is obtained by changing the position of the bead along one direction, say the x direction, by moving the trapping IR laser with a mirror. The maximum backscattered intensity occurs when the IR laser, He-Ne laser and detector are all aligned. The secondary peaks located at about $(R/2)$, where R is the radius of the bead, are due to internal reflections inside the bead, since the peak at the left occurs when we move the bead to the left and vice versa. The bead used in this run was a Polyscience bead, stock number No. 452308. For a bead manufactured by the same company, same specifications, but another stock (No. 500816), the scattering profile is very different as compared to the previous one (crosses in Fig. 3). Therefore if we intend to make quantitative measurements using such scattering profiles we have to measure them for each bead used in an

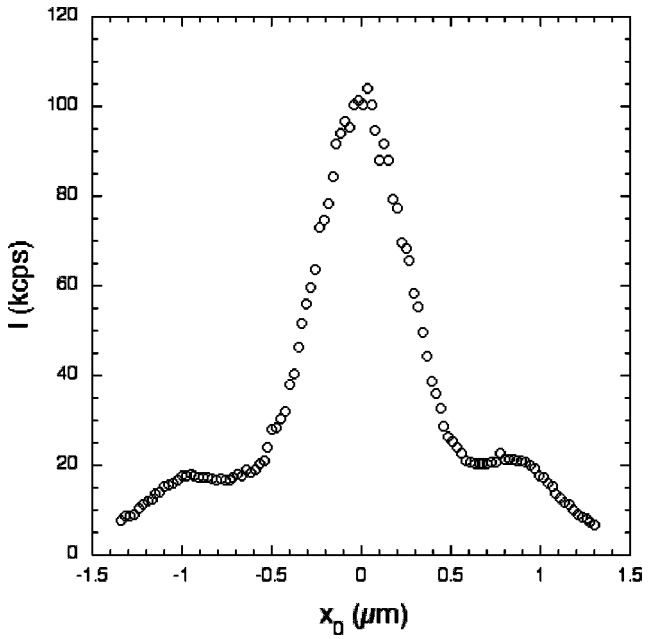

FIG. 2. Backscattering intensity profile with the photodetector collinear to the He-Ne laser for Polyscience bead stock No. 452308. x_0 is the bead center position in relation to the He-Ne laser. Secondary peaks are due to internal reflections inside the bead.

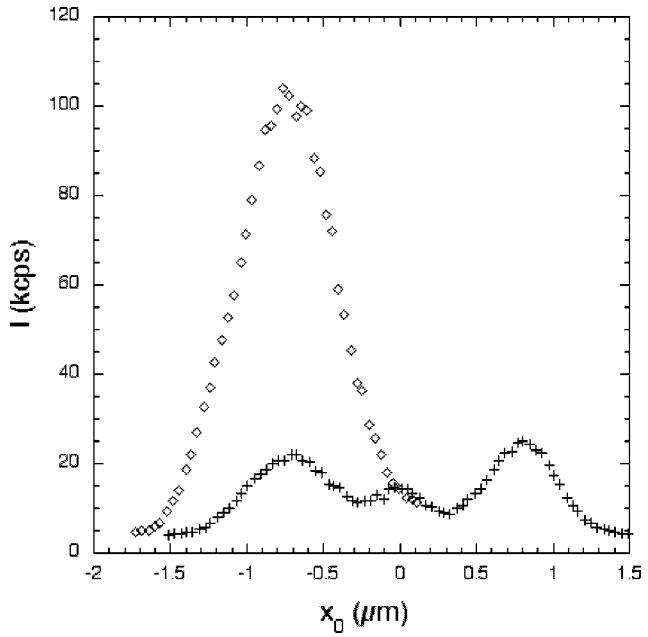

FIG. 3. Crosses: Same as in Fig. 2 but with Polyscience bead stock No. 500816. Diamonds: The photodetector is positioned to maximize the left secondary peak.

experimental run. The diamonds in Fig. 3 represent the same profile as that represented by crosses, but with the photodetector displaced towards the secondary peak at left. The intensity of this secondary peak increases and becomes as large as, or even higher than, the central peak of the previous profile. Our experiments are carried out with this geometry because the secondary peak intensities are more reproducible and the photodetector is no longer aligned with the He-Ne laser, which prevents back reflected light from the coverslip of the sample cell to hit the photodetector. We can measure the two-dimensional backscattering profile by moving the bead along both x and y directions. In our geometry it is not possible to change the position of the bead along z in relation to the position of the He-Ne laser, since both IR and He-Ne lasers are focused by the same microscope objective. Therefore, the z position of the bead is fixed by the geometry and it is very close to the focal point. We can vary the x and y position of the bead in relation to the incident He-Ne laser by moving the IR trapping laser beam.

A. Temporal-intensity-autocorrelation function (ACF) for Gaussian profiles

Let us assume initially that the scattering profile is a pure anisotropic Gaussian function in three-dimensions:

$$I(x,y,z)=I_0\exp\left(-\frac{x^2}{2\sigma_x^2}\right)\exp\left(-\frac{y^2}{2\sigma_y^2}\right)\exp\left(-\frac{z^2}{2\sigma_z^2}\right). \tag{1}$$

The scattering profiles can be slightly asymmetric as shown in Fig. 3, and it is in fact a Lorentzian along z. Later we shall deal with more realistic profiles. If the average position of the bead is (x_0,y_0,z_0) it executes a bound Brownian motion around this position. Therefore, at each instant the particle position is $[x_0+\Delta x(t),y_0+\Delta y(t),z_0+\Delta z(t)]$, and the backscattered intensity $I[x_0+\Delta x(t),y_0+\Delta y(t),z_0+\Delta z(t)]$ fluctuates in time accordingly. The $\Delta x(t)$, $\Delta y(t)$, and $\Delta z(t)$ are Gaussian stochastic variables with zero mean values. Following the procedure of Bar-Ziv *et al.* [7] to calculate the temporal-intensity autocorrelation function, we obtain the general expression

$$\langle I(\Delta x_i)I(\Delta x_i')\rangle = I^2(x_{0i})\prod_i \frac{\sigma_i^2}{\sqrt{(\langle\Delta x_i^2\rangle+\sigma_i^2)^2-\langle\Delta x_i\Delta x_i'\rangle^2}} \times\exp\left[-\frac{x_{0i}^2}{(\langle\Delta x_i^2\rangle+\sigma_i^2+\langle\Delta x_i\Delta x_i'\rangle)}\right], \tag{2}$$

where $x_{01}=x_0$, $x_{02}=y_0$, $x_{03}=z_0$, $\sigma_1=\sigma_x$, $\sigma_2=\sigma_y$, $\sigma_3=\sigma_z$, $\Delta x_1=\Delta x$, $\Delta x_2=\Delta y$, and $\Delta x_3=\Delta z$. By setting $x_0=0$, $y_0=0$, and $z_0=0$ we obtain the expression of Bar-Ziv *et al.* [7]. An important point in our more general expression is that for x_0, y_0, and z_0 different than zero, both first-order and second-order temporal correlations of the particle position are present. Such a mixture can be a problem when determining the decay time of position fluctuations, since we may have exponential functions with decay times differing by a factor of 2 and with variable amplitudes. This effect resembles the annoying problem in standard QEDLS where spurious local oscillator laser light could result in a mixture of homodine and heterodine signals [6]. However, we can use this fact in our favor, since here we can easily control the amount of each component by positioning the bead in a convenient location in relation to the scattering profile maximum. As a consequence we can improve signal-to-noise ratios selectively for x or y position fluctuations. A good way for checking if one has first or second-order correlations is to oscillate the sample cell and consequently the bead with a known frequency: if one has a first-order correlation the resulting ACF will oscillate with the same frequency as the bead. If one has a second-order correlation, the ACF will oscillate with twice this frequency.

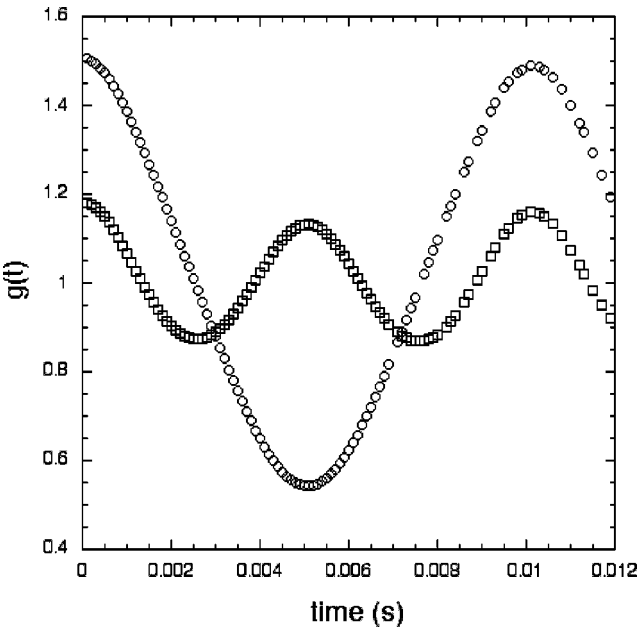

FIG. 4. Circles: ACF of a bead oscillating at 100 Hz with amplitude of ~ 0.3 μm around the position $x_0=0.3$ μm. Squares: Same as above but with the bead oscillating around $x_0=0$ (second-order ACF).

The circles in Fig. 4 represent an ACF of a trapped bead oscillating at 100 Hz along the x direction, amplitude of order 0.3 μm and x_0 of order 0.3 μm. The squares in Fig. 4 represent the same oscillation but with the bead centered at the maximum of the scattering profile, i.e., $x_0=0$. We see that for $x_0=0.3$ μm we have first-order correlation and for $x_0=0$ second-order correlation. This result is easy to understand because if the oscillating bead is far from the profile peak, the scattered intensity will return to the same value when the particle returns to its initial position (after one cycle). On the other hand, a centered bead will pass through two positions with the same scattered intensity for each cycle, consequently the ACF will have a frequency that is twice that of the bead. We shall see later that, even for amplitudes compared to typical Brownian amplitudes (in our

case 50 nm at most), we will use the ratio between the amplitudes of the oscillating first- and second-order correlations to make sure that the bead is well centered, say in relation to the y axis and off centered in relation to the x axis. In this way we select which fluctuations Δx or Δy we are going to probe.

B. Position correlation function of a harmonically bound Brownian particle

If a particle is confined in a harmonic potential well, like in the case of our bead trapped by an optical tweezer, this particle will execute a Brownian motion confined to the potential well. We can write a Langevin equation for this problem:

$$m\ddot{x}_i+\gamma\dot{x}_i+k_i x_i=f(t),$$

where m is the mass of the bead, the friction coefficient is $\gamma=6\pi\eta R$, with η the viscosity of the surrounding medium and R the bead radius, k_i are the curvatures of the potential energy or stiffnesses along each direction, and $f(t)$ is a stochastic force that satisfies

$$\langle f(t)f(t')\rangle=2\gamma k_B T\delta(t-t')$$

and

$$\langle f(t)\rangle=0,$$

where k_B is the Boltzmann constant and T the absolute temperature.

In our experiments we use polystyrene beads with $R=1.4\times10^{-4}$ cm and density $\rho=1.05$ g/cm^3 in water with $\eta\simeq10^{-2}$ Poise. Stiffnes of the optical tweezer varies from 10^{-3} to 10^{-2} dyn/cm. Since $(\gamma/m)\gg\sqrt{k/m}$, the motion of the bead is strongly damped and there are two decay times: $\tau_{\text{fast}}=m/\gamma\simeq10^{-6}$ s and $\tau_{\text{slow}}=\gamma/k\simeq10^{-2}$ to 10^{-3} s. By performing an average over the fast time scale one obtains [8]

$$\langle\Delta x_i(0)\Delta x_i(t)\rangle=\langle\Delta x_i^2\rangle\exp(-t/\tau_i), \tag{3}$$

where

$$\langle\Delta x_i^2\rangle=k_B T/k_i \tag{4}$$

and

$$\tau_i=\frac{\gamma}{k_i}. \tag{5}$$

For a Gaussian process:

$$\langle\Delta x_i^2(0)\Delta x_i^2(t)\rangle=\langle\Delta x_i^2\rangle^2+2\langle\Delta x_i(0)\Delta x_i(t)\rangle^2,$$

$$\langle\Delta x_i^2(0)\Delta x_i^2(t)\rangle=\langle\Delta x_i^2\rangle^2\left[1+2\exp\left(-\frac{2t}{\tau_i}\right)\right]. \tag{6}$$

C. ACF for an optically trapped bead for a general profile: Strong trap limit

To obtain the general ACF for an optically trapped bead we substitute the results from Eqs. (3)–(6) into Eq. (2). This result is valid even if the Brownian amplitudes are larger than the backscattering Gaussian widths. If the Gaussians are distorted, or if the profile is not a Gaussian, this analysis is not valid. In many situations of interest, the optical tweezers stiffness in the x and y directions (transverse stiffness) are larger than 5×10^{-3} dyn/cm. Along the z direction the stiffness (axial stiffness) is about 7 times smaller than the transverse stiffness, since for the IR laser $\sigma_x\simeq\sigma_y\simeq\sigma_z/7$ as well. Therefore, using Eq. (5) we obtain that $\sqrt{\langle\Delta x_i^2\rangle}/\sigma_i\leqslant0.1$, such that the amplitude of the fluctuations is much smaller than the width of the He-Ne laser backscattering profile (strong trap limit). Then, we can derive an approximate ACF, that is valid for more general profiles, by making a Taylor series expansion of the backscattering profile about a particular average position of the bead. With this procedure we gain simplicity and the possibility of analyzing more realistic backscattering profiles. A more general backscattering profile can be written as

$$I(x,y,z)=I_0\exp[-f(x,y,z)]. \tag{7}$$

Expanding this intensity profile in Taylor series about the position x_0,y_0,z_0 we obtain up to second order

$$I(\Delta x_i)=I(x_{0i})\left\{1+\sum_i\left(\alpha_i\Delta x_i+\beta_i\Delta x_i^2\right)\right\}, \tag{8}$$

where

$$I(x_{0i})=I_0\exp[-f(x_{0i})], \tag{9}$$

$$\alpha_i=\left(-\frac{\partial f}{\partial x_i}\right)_{x_{0i}}, \tag{10}$$

and

$$\beta_i=\frac{1}{2}\left[\left(\frac{\partial f}{\partial x_i}\right)_{x_{0i}}^2-\left(\frac{\partial^2 f}{\partial x_i^2}\right)_{x_{0i}}\right]. \tag{11}$$

Since $\langle\Delta x_i\rangle=0$ and $\langle\Delta x_i\Delta x_j\rangle=0$ for $i\neq j$, we obtain the approximate ACF,

$$\langle I(\Delta x_i)I(\Delta x_i')\rangle = I(x_{0i})^2\Bigg[1+\sum_i\ [\beta_i\langle(\Delta x_i)^2\rangle + \alpha_i^2\langle\Delta x_i\Delta x_i'\rangle+\beta_i^2\langle(\Delta x_i)^2(\Delta x_i')^2\rangle]\Bigg]. \tag{12}$$

For our purposes, we can simplify this expression even further. Let us make some numerical estimates for a Gaussian backscattering profile. In this case

$$\alpha_i=\left(-\frac{\partial f}{\partial x_i}\right)_{x_{0i}}=-\frac{x_{0i}}{\sigma_i^2}$$

and

$$\beta_i=\frac{1}{2}\left[\left(\frac{x_{0i}}{\sigma_i^2}\right)^2-\frac{1}{\sigma_i^2}\right].$$

We notice that the first-order ACF is null at the profile peak while the second-order ACF is null at $x_{0i}=\sigma_i$. Therefore, if we keep the bead position smaller than $2\sigma_i$, the first-order ACFs will have magnitude much larger than the second-order ACF if $x_{0i}\gg\sqrt{\langle\Delta x_i^2\rangle}/2$. For bead average positions x and $y>15$ nm and $z>90$ nm we then basically measure first-order ACFs. For comparison with the theory we will keep $\alpha_x\gg\beta_x$ and $\alpha_y=0$ in our experiments, then we make sure that we are looking only at the Brownian fluctuations along the x direction. Since the motion along the z direction is much slower than the motion along the x direction (because $k_z\ll k_x$), it can be easily separated out in the measured ACF. In addition, within the range considered and for $\sqrt{\langle\Delta x_i^2\rangle}/\sigma_i\leqslant 0.1$, the quantity $\Sigma_i\beta_i\langle(\Delta x_i)^2\rangle\simeq 1.5\times10^{-2}$ at the worst situation ($x_0=y_0=z_0=0$), which is negligible compared to unity, therefore from Eq. (8), $\langle I(\Delta x_i)\rangle\cong I(x_{0i})$. Finally, we write down our first-order normalized ACF as

$$g(t)=\frac{\langle I(\Delta x_i)I(\Delta x_i')\rangle}{\langle I(\Delta x_i)\rangle^2},$$

$$g(t)=1+\alpha_x^2\langle\Delta x\Delta x'\rangle+\alpha_z^2\langle\Delta z\Delta z'\rangle,$$

$$g(t)=1+\alpha_x^2\langle\Delta x^2\rangle\exp\left(-\frac{t}{\tau_x}\right)+\alpha_z^2\langle\Delta z^2\rangle\exp\left(-\frac{t}{\tau_z}\right). \tag{13}$$

Given the restrictions discussed above, Eq. (13) can be applied to any scattering profile. Therefore, if we measure the backscattering profile and measure the ACF we have enough information to obtain the amplitudes and decay times of the Brownian motion of the trapped bead. An example of a measured ACF fitted with Eq. (13) is shown in Fig. 5. If the profile is a pure Gaussian as given in Eq. (1), $\alpha_x^2=x_0^2/\sigma_x^4$ and $\alpha_z^2=z_0^2/\sigma_z^4$, then Eq. (13) can be written as

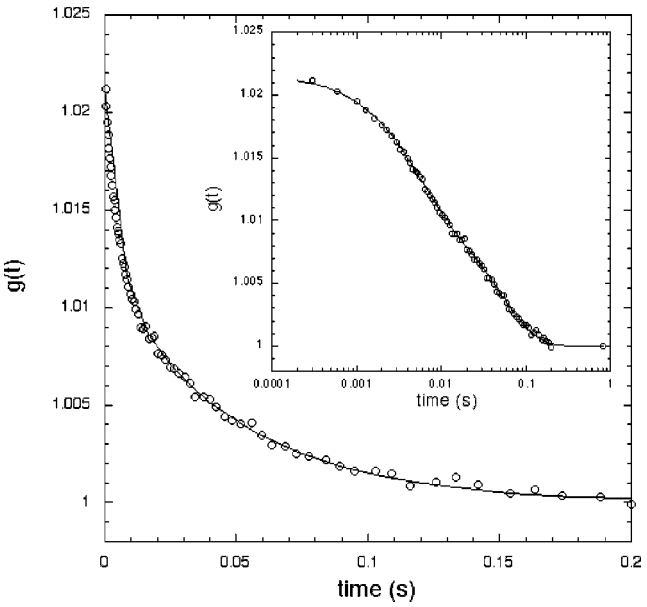

FIG. 5. Typical normalized ACF function fitted to $g(t)=1+A_x\exp(-t/\tau_x)+A_z\exp(-t/\tau_z)$; $\tau_z\approx 7\tau_x$. Inset: Same ACF in a semilog plot showing delayed channels.

$$g_G(t)=1+\frac{x_0^2}{\sigma_x^4}\langle\Delta x^2\rangle\exp\left(-\frac{t}{\tau_x}\right)+\frac{z_0^2}{\sigma_z^4}\langle\Delta z^2\rangle\exp\left(-\frac{t}{\tau_z}\right). \tag{14}$$

The non-normalized ACF is then

$$G_G(t)=[I_0\exp(-x_0^2/2\sigma_x^2)\exp(-z_0^2/2\sigma_z^2)]^2\times\left[1+\frac{x_0^2}{\sigma_x^4}\langle\Delta x^2\rangle\exp(-t/\tau_x)+\frac{z_0^2}{\sigma_z^4}\langle\Delta z^2\rangle\exp(-t/\tau_z)\right], \tag{15}$$

and finally

$$G_{\text{integral}}(t)=\int_{-\infty}^{+\infty}G_G(x_0,0,z_0,t)dx_0=\text{const}\ \ g_{\text{integral}}(t),$$

where

$$g_{\text{integral}}(t)=\left[1+\frac{1}{2\sigma_x^2}\langle\Delta x^2\rangle\exp(-t/\tau_x)+\frac{z_0^2}{\sigma_z^4}\langle\Delta z^2\rangle\exp(-t/\tau_z)\right]. \tag{16}$$

The important difference between Eqs. (14) and (16) is the factor multiplying $\exp(-t/\tau_x)$. Later we will describe two experimental methods: the differential method measures $g(t)$ and the integral method measures $g_{\text{integral}}(t)$. We shall discuss the advantages and disadvantages of each one.

III. EXPERIMENTS

A. Experimental setup

The experimental setup is shown in Fig. 1. An inverted optical microscope Nikon TE300 with an infinity corrected objective (100X, N.A.=1.4) is used to make the optical tweezer, observe the bead and collect the scattered intensity. In one port of the microscope we use a CCD camera (CCD-72 DAGE-MTI) for visualization. In another port we use a photodetector (EG&G-Photon Counting Module, SPCM-200-PQ-F500), with collection diameter of 150 μm mounted in Newport XY stages to be precisely positioned. The EG&G photodetector delivers TTL pulses ready to be fed into a Brookhaven BI-9000AT digital correlator. An IR laser (SDL, 5422-H1) operating at 830 nm, with maximum power of 150 mW is used for the optical tweezer. The light of a He-Ne laser (SP-127) is the scattering probe. A line filter for wavelength 632.8 nm is put in front of the photodetector to eliminate the IR and any light other than the He-Ne laser light. A half-wave plate and polarizers are used to control the intensity and polarization of the He-Ne incident and scattered lights. The microscope stage was substituted by Newport XY stages driven by piezoelectric actuators. The calibration of the motion of the stages was done using a Fabry-Perot interferometer built in such a way that a mirror was fixed on one stage and another mirror fixed on the microscope. This interferometer could be switched from the X stage to the Y stage. This calibration was periodically checked. A micromotor (m) was connected to the mirror ($M1$) that drives the IR laser on the objective. The purpose of this motor is to move the IR beam and, consequently, move the trapped bead in relation to the fixed He-Ne laser beam to obtain the backscattering profile as a function of time. From an accurate measurement of the bead speed, time is converted into position and one gets the backscattering profile as a function of position. The motion of the bead was recorded with the CCD camera. Images were analyzed, and the bead speed was then extracted. The image pixel size was measured by recording the motion of a bead stuck on the microscope slide and driven by one of the previous calibrated stages. Thus, all lengths were calibrated using a Fabry-Perot interferometer. Samples were made with polystyrene spheres of diameter 2.8 μm (Polyscience) in deionized water. The setup was mounted on a homemade isolating table.

B. Experimental procedure

1. Measurement of the backscattering profile

The backscattering profile is measured by moving the IR laser beam along the x or y direction, and consequently moving the trapped bead in relation to the fixed He-Ne laser beam. Typical profiles are shown in Figs. 2 and 3. These profiles have a central peak and two secondary peaks. The central peak has great variability from bead to bead. For some beads, the central peak has its maximum intensity when the IR beam, He-Ne beam and photodetector are all aligned (Fig. 2). For some other beads the central peak is very weak (crosses in Fig. 3). Secondary peak intensities, that we believe come from internal reflections inside the bead, are more reproducible. By changing the position of the photodetector their intensities can be maximized, and can become even stronger than the intensity of the central peak in the previous situation (diamonds in Fig. 3). All of our experiments were performed with the photodetector positioned such as to maximize one of the lateral peaks intensity. They change less from one bead to another and the photodetector (out of center) does not collect light directly reflected from the microscope glass slide. In addition, much of the stray light from other reflections and from spurious scattering in the medium can be avoided by collecting the light cross polarized with the incident He-Ne beam. It is also advisable to have the same intensity of the IR laser during the measurement of the backscattering profile as that during ACF measurements. In order to have the maximum contribution to ACFs due to motion of the bead along the x direction and minimum along the y direction, we have to be sure that the bead is centered in relation to the y direction. We guarantee this by oscillating the stage along the y direction, causing a motion of the bead, with amplitude comparable to that of the Brownian amplitude. By measuring oscillatory ACFs along the y direction (similar to the ones in Fig. 4) we minimize their amplitudes while we slightly move the photodetector. When a minimum amplitude comparable to what is expected from a second-order ACF is obtained we know that $y_0=0$. We check that for different positions x_0. Under these conditions a typical profile along the x direction is shown in Fig. 6. In this case the IR laser intensity was around 6 mW (at the bead). The IR beam and the bead moved at a speed of 0.0138 ± 0.0004 μm/s, such that a Stokes force of 0.01 pN causes negligible displacements of the bead in relation to the potential well center. Later, this profile will be used for analysis of the data from measured ACFs as a function of x_0.

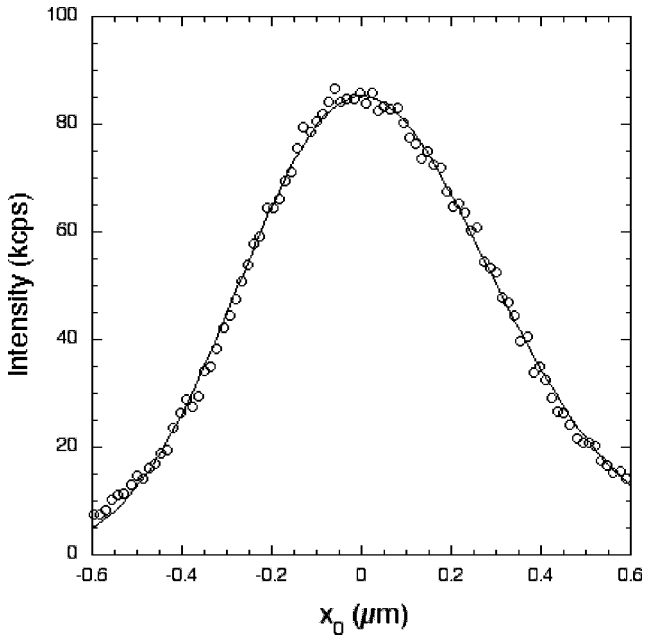

FIG. 6. Backscattering intensity profile fitted using the function $I_0 \exp[-(x_0^2/2\sigma_x^2 - c_x x_0^3)]$, with $\sigma_x = 0.276 \pm 0.008$ μm and $c_x = 2.1 \pm 0.1$ μm^{-3}. This profile was used to illustrate the differential method.

2. Measurement of ACFs: Differential method

ACFs are measured with the digital correlator. The trapped bead is positioned in a particular position x_0 and $y_0=0$ of the backscattering profile, as described earlier. At this fixed position an ACF is recorded. A typical ACF is shown in Fig. 5, where only 50% of the experimental points are shown.

This ACF is normalized by the average intensity of that run (correlator delayed channels). The ACF is fitted with Eq. (13), and the two time constants (τ_x and τ_z) and their amplitudes ($A_x=\alpha_x^2\langle\Delta x^2\rangle$ and $A_z=\alpha_z^2\langle\Delta z^2\rangle$) are then obtained. We measure a set of ACFs as a function of the x_0 position of the bead in relation to the peak of the scattering function. The bead is located 10 μm above the cell bottom. The time constant τ_z is around 6 to 10 times larger than τ_x and fluctuates from one measurement to another. This variation may be caused by our imprecise control of the bead position in relation to the z direction. Therefore, since the bead is close to the focus of the laser, it is close to the peak center. Thus, along the z direction we are probably measuring a mixture of second and first-order ACFs, with variable amounts of each one. Since these two time scales τ_z and τ_x are well separated, we concentrate our analysis on the motion along the x direction. By measuring the profile along the x direction and from the measurement of A_x, we can obtain the tweezer's transverse stiffness. If the friction is known then the transverse stiffness can also be obtained from the decay time of ACFs. In this case, for consistency the value of the transverse stiffness obtained from the amplitude of the ACFs has to agree with the value obtained from the decay time of ACFs. The method described here allows us to selectively measure the stiffness of the optical tweezer along the three directions k_x and k_y can be selectively measured by positioning adequately the bead on the scattering profile; k_z might, in principle, be obtained from the long time constant of ACFs.

3. Measurement of ACFs: Integral method

In this method a single ACF is accumulated while the particle slowly moves with constant speed along the scattering profile. Therefore, an integration of the ACF in relation to x_0 is performed. This method is much faster than the differential one. Because of the long average in both time and position, and since the ACF is collected simultaneously with the backscattering profile, this method returns more stable results. A typical particle speed used is 3 nm/s. This method is more easily implemented if the scattering profile along the x axis can be fitted by a single Gaussian. In this case we can use Eq. (16) to fit the ACF and since we have σ_x from the backscattering profile, we can obtain k_x from the amplitude of the ACF and the friction coefficient from the decay time. For a more complex profile, the same information can be obtained, however, it would involve a more extensive data analysis. Therefore, we prefer to fine adjust the photodetector's position until we get a good Gaussian profile and then use the integral method described here.

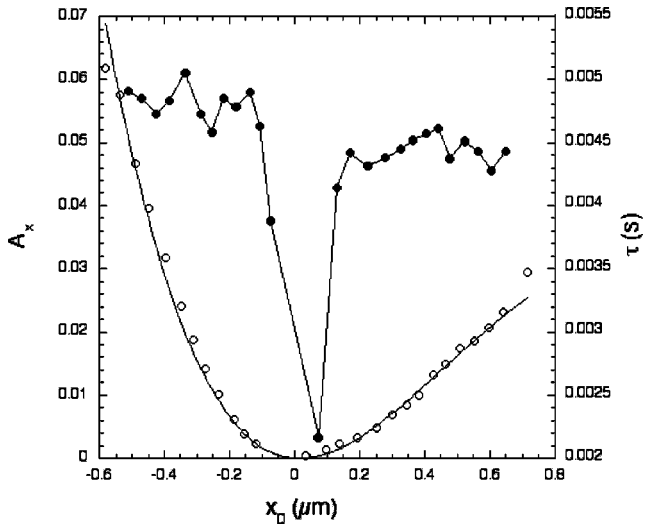

FIG. 7. Empty circles: Values for the first-order ACF amplitudes as a function of the bead position x_0 in relation to the maximum of the backscattering profile. The continuous line is a fit using $A_x=(x_0/0.276^2-6.3x_0^2)^2\langle\triangle x^2\rangle$ with $\langle\triangle x^2\rangle$ as a free parameter. From the best fit $\langle\triangle x^2\rangle=(6.8\pm0.2)\times10^{-4}$ μm^2. Filled circles: Values for the decay time τ_x as a function of x_0. Near $x_0=0$, τ_x drops to half of its value, indicating a second-order ACF as expected from the theory.

IV. RESULTS AND DISCUSSION

A. Differential method

We position the bead on the scattering profile in such a way to measure the motion along the x and z directions. We collect the cross-polarized backscattered light. A backscattering profile obtained along the x direction and at $y_0=0$ is shown in Fig. 6.

By improving the position of the photodetector we can obtain backscattering profiles that are single Gaussians. We, however, used the slightly distorted profile of Fig. 6 to illustrate this more general approach. The amplitudes ($A_x=\alpha_x^2\langle\Delta x^2\rangle$) and time constants ($\tau_x$) of the measured ACFs [fitted using Eq. (13)] as a function of x_0 are shown in Fig. 7.

As one would expect, the minimum amplitude occurs for $x_0=0$ and the time constant measured in this position is about half of the value far from the peak (second-order ACF). We fit the profile of Fig. 6 to $I(x_0,y_0,z_0)=I_0\exp[-f(x_0,y_0,z_0)]$ as a function of x_0, with $y_0=0$ and z_0 fixed. From the fit we obtain $f(x_0,0,0)=x_0^2/2\sigma_x^2-c_x x_0^3$, with $\sigma_x=0.276\pm0.008$ μm and $c_x=2.1\pm0.1$ μm^{-3}. Since $\alpha_x=\partial f/\partial x_0=x_0/\sigma_x^2-3c_x x_0^2$, the amplitude $A_x=\alpha_x^2\langle\Delta x^2\rangle$ can be written as $A_x=\alpha_x^2\langle\Delta x^2\rangle=(x_0/0.276^2-6.3x_0^2)^2\langle\Delta x^2\rangle$. We then fit the curve for $A_x\times x_0$ using this expression with $\langle\Delta x^2\rangle$ as the only fitting parameter. From this fit we obtain $\langle\Delta x^2\rangle=(6.8\pm0.2)\times10^{-4}$ μm^2 that results in $k_x=0.0059\pm0.0004$ dyn/cm, while the value obtained from the average decay time of the first-order ACF is $k_x=0.0058\pm0.0002$ dyn/cm, with very good agreement. We used $\gamma=1.08\gamma_0$, where $\gamma_0=6\pi\eta R$, with $\eta=0.902\times10^{-2}$ Poise (25 °C) and $R=1.4\times10^{-4}$ cm. This correction to the friction coefficient is needed because of the finite bead distance

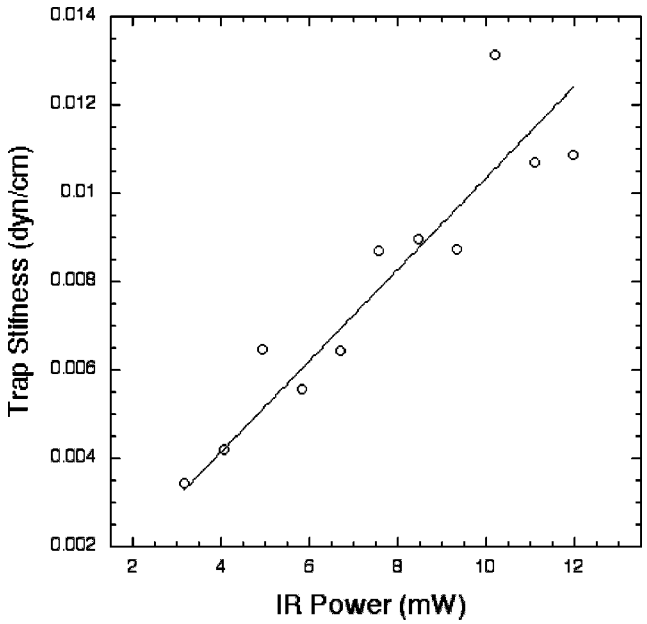

FIG. 8. Circles: Values for the transverse stiffness as a function of the infrared laser power at the trapped bead. Continuous line: Straight line fit as predicted by theory (slope equal to 1.0 ± 0.1 dyn/W cm).

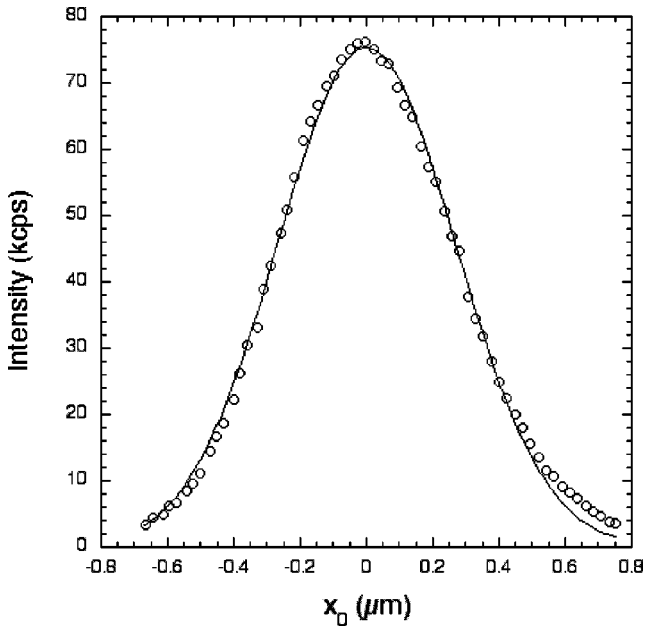

FIG. 10. Backscattering intensity profile fitted to a single Gaussian with $\sigma_x = 0.268 \pm 0.008$ μm, used to illustrate the integral method.

($h = 10$ μm) to the coverslip, as we will discuss in Sec. V. This result indicates that we have good control over this technique and we can safely use it for applications. In Fig. 8 we plot the trap transverse stiffness as a function of the IR laser incident power on the bead, which should be a linear function [2].

By moving the sample cell stage with a fixed speed V along the x direction, the trapped particle experiments a frictional Stokes force given by $F_{\text{Stokes}} = \gamma V$. The particle position changes from its original equilibrium position to a new one such that the trap force $F_{\text{trap}} = k_x \Delta x$ has to equilibrate the Stokes force. The displacement Δx can be obtained from the backscattering profile since there is a correspondence between backscattered intensity and position of the bead. In equilibrium $F_{\text{Stokes}} = F_{\text{trap}}$. Since we know γ we can calculate the Stokes force for different speeds V and measure the correspondent Δx. We can use the value of k_x obtained by the previous method to obtain the trap force. Therefore, for

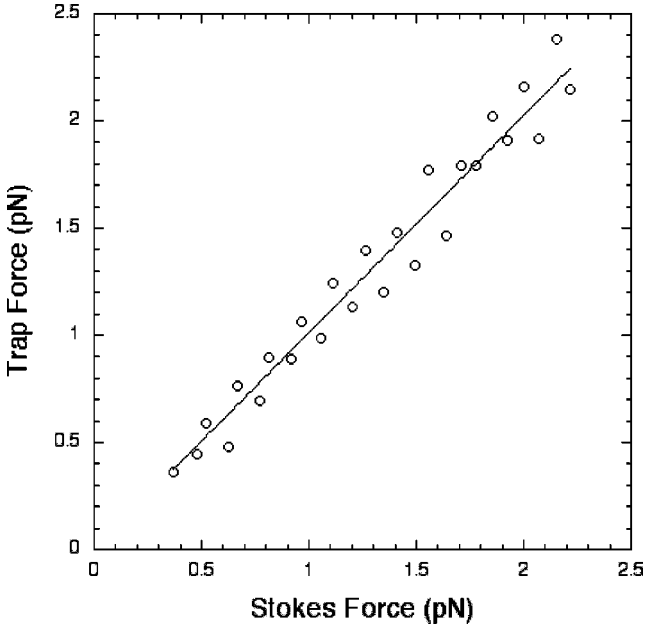

FIG. 9. Calibration of the tweezer's trapping force using the Stokes force method as described in the text. The straight line has slope very close to unity (1.01), indicating the consistency of the calibration methods.

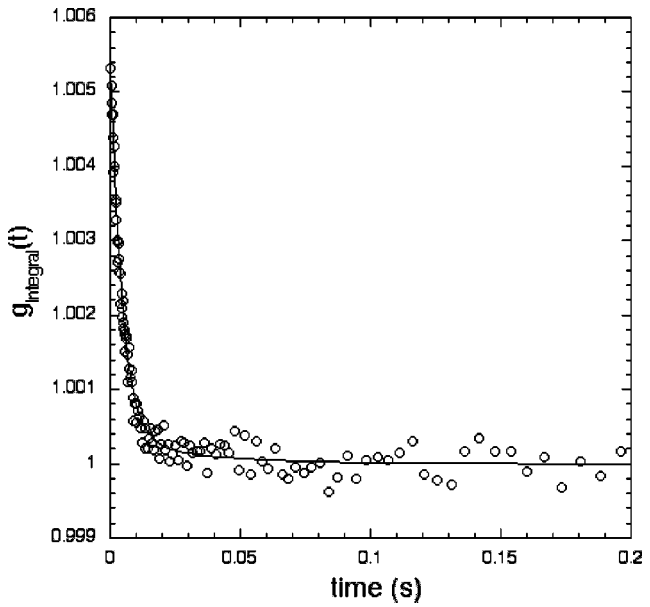

FIG. 11. Integrated ACF fitted to Eq. (16), illustrating the integral method as described in the text.

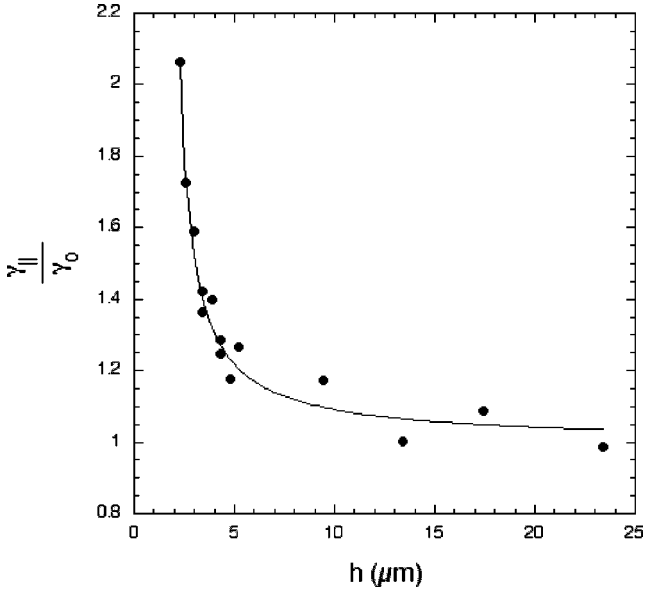

FIG. 12. Circles: Values of the parallel Stokes friction on the trapped bead normalized to $\gamma_0 = 6\pi\eta R$, as a function of the distance h from the coverslip. Continuous curve: Fit using Eq. (17) with a initial height correction of $h_0 = 0.65$ μm, as described in the text.

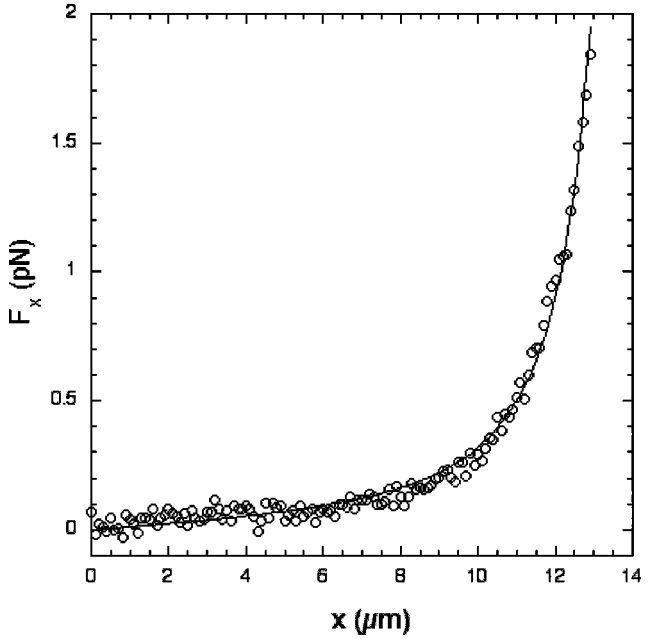

FIG. 13. Circles: Values for the x component of the entropic force of a single λ-DNA molecule as a function of x in a stretching experiment. Continuous curve: Fit using the Marko and Siggia model for the DNA entropic force. From the fit one obtains a persistence length ($A = 41.8 \pm 0.8$) nm and a contour length ($L = 15.55 \pm 0.02$) μm.

consistency, in a plot of $F_{trap} \times F_{Stokes}$ we should obtain a straight line with unity slope (Fig. 9). In our case the slope obtained is equal to 1.01. The Stokes force method is commonly used for optical tweezers calibration [5]. From ACF and backscattering profile measurements, both the transverse stiffness and the friction coefficient γ on a trapped sphere can be obtained.

B. Integral method

As mentioned before, the integral method is easier to use with a good Gaussian profile. In Figs. 10 and 11 we show a typical profile and the integrated ACF.

These data were obtained at $h = 20$ μm and temperature of 26.8 °C. The stiffnesses obtained from the decay time and from the amplitude of the exponential are $k_x = 0.0055 \pm 0.0003$ dyn/cm and $k_x = 0.0054 \pm 0.0002$ dyn/cm indicating that the method is consistent. We will use both methods for the two applications to be discussed in the next section.

V. APPLICATIONS

A. Parallel Stokes friction as a function of height

As an application of the integral method developed above we will measure the parallel Stokes friction coefficient on the microsphere as a function of the distance from the microscope coverslip. The Stokes force increases as the microsphere approaches the surface of the slide. In 1991 we performed such measurements using QELS. The theoretical background and the expression for the Stokes force can be found in Feitosa and Mesquita [9]. Such measurements were also performed by other groups [10,11]. We revisit this problem to show an application of the above technique. Since the laser profile may change as we vary the focal distance in relation to the coverslip it is necessary, in each run, to measure the tweezer's transverse stiffness from the ACF amplitude and from its decay time to obtain the parallel friction coefficient. An expression for the parallel friction coefficient is given by

$$\frac{\gamma_{//}}{\gamma_0} = \left[1 - \frac{9}{16}\left(\frac{R}{h}\right) + \frac{1}{8}\left(\frac{R}{h}\right)^3 - \frac{45}{256}\left(\frac{R}{h}\right)^4 - \frac{1}{16}\left(\frac{R}{h}\right)^5\right]^{-1}, \tag{17}$$

where $\gamma_0 = 6\pi\eta R = 2.27 \times 10^{-5}$ dyn s/cm, with $\eta = 0.859$ Poise (26.8 °C) is the water viscosity, $R = 1.4$ μm, is the microsphere radius and h is the distance from the microsphere center to the cover slip. The height h can be varied by moving the microscope objective in relation to the cover slip, since the focal point and, consequently, the position of the bead is varied. By moving the objective with the microscope knob (with divisions of one micron) we know the variation of height, but not the initial height. In order to obtain it we move the objective until the bead touches the coverslip. At this point the height is close to the bead radius. With this procedure an error of about 0.5 μm in the initial value for h is likely to occur. We normalize the measured data for $\gamma_{//}$ by γ_0 and fit the data using Eq. (17), where the initial height is the only adjustable parameter. To do that, we replace h by $h - h_0$ in Eq. (17). In Fig. 12 we show the data and the fit to Eq. (17). The height correction that comes from the fit is $h_0 = 0.65$ μm.

B. Entropic elasticity of DNA

By attaching one end of a single λ-DNA molecule to a 2.8 μm polystyrene microsphere and the other end to a microscope cover slip, following the procedure of Shivashankar *et al.* [12], we can keep the microsphere trapped with the optical tweezer and move the cell stage to stretch the DNA. The DNA sample is a PBS solution with $pH=7.4$ and $[Na]=150$ mM. At the unstretched configuration, the bead is at the equilibrium position in relation to the tweezer's potential. We positioned the bead at a height of 5 μm above the cover slip. At this height the DNA is only stretched by 5 μm, such that its stiffness is much smaller than the tweezer's transverse stiffness. Therefore, by measuring ACFs and knowing the friction coefficient at this height, we can obtain the tweezer's transverse stiffness. Then we move the cell stage very slowly (~ 0.054 μm/s) and record the backscattered intensity. Since we had previously measured the backscattering profile, again we can obtain the bead displacement as the DNA molecule is stretched. From the product of the tweezer's transverse stiffness ($k_x=0.0080\pm 0.0003$ dyn/cm for this run) by the bead displacement we can obtain the instantaneous force along the x direction due to the DNA. A plot of the x component of the DNA entropic force as a function of x is shown in Fig. 13.

In order to diminish the Brownian noise, the data in Fig. 13 corresponds to an average over four runs for the same bead and same DNA. Marko and Siggia have derived an expression for the DNA entropic force as a function of its elongation [13], given by

$$F_{\mathrm{DNA}}=\frac{k_BT}{A}\left[\frac{z}{L}+\frac{1}{4\left(1-\frac{z}{L}\right)^2}-\frac{1}{4}\right], \tag{18}$$

where k_B is the Boltzmann constant, T is the absolute temperature, A is the DNA persistence length, L is the DNA contour length, and z is the DNA end-to-end separation. The x component of the DNA entropic force as a function of x can be written as

$$F_x=\frac{k_BT}{A}\left[\frac{\sqrt{x^2+h^2}}{L}+\frac{1}{4\left(1-\frac{\sqrt{x^2+h^2}}{L}\right)^2}-\frac{1}{4}\right]\frac{x}{\sqrt{x^2+h^2}}. \tag{19}$$

The data in Fig. 13 is fitted using Eq. (19), with $h=5$ μm and A and L as free parameters. The result is $A=(41.8\pm 0.7)$ nm and $L=(15.55\pm 0.03)$ μm. These error bars are for this set of curves. For other runs the average value of A is about 42 nm with an overall error of ± 2 nm. These values are in agreement with the literature [3,5]. The contour length L for λ-DNA is listed to be 16.5 μm. We have found lengths that vary from 13 to 22 μm.

VI. CONCLUSIONS

We have presented a thorough account on the dynamic light scattering from a microsphere trapped by optical tweezers. The results are fully consistent with the theory of the Brownian motion of a harmonically bound particle. By measuring the backscattering profile and ACFs, we obtain the amplitude and decay time of the Brownian motion of the microsphere. From the amplitude we obtain the transverse stiffness of the optical tweezer. From the decay time, we can also obtain the transverse stiffness if we know the friction coefficient of the bead, checking the consistency of the method. Or since we know the stiffness we can obtain the friction on the bead if it is unknown. Thus, with this technique we can obtain simultaneously the stiffness and the friction on the bead. It has potential applications in rheological studies of viscoelastic media. We showed two applications of the method developed here: in the first (measurement of parallel Stokes friction as a function of height), we obtain the tweezer's stiffness from the ACF amplitude and the friction on the bead from the decay time. In the second (measurement of λ-DNA entropic elasticity), we obtain the tweezer's transverse stiffness from the decay time of ACFs and by knowing the backscattering profile we can measure the displacement of the bead in relation to its equilibrium position, when the DNA molecule attached to the bead is stretched. From the product of the trap stiffness by bead displacement we obtain the DNA entropic force as a function of its elongation. Results are in good agreement with the literature values, indicating that the method developed here can be consistently used.

ACKNOWLEDGMENTS

We acknowledge helpful discussion with A. Libchaber and G. V. Shivashankar and also S. P. Walborn for a critical reading of the manuscript. This work was supported by the Brazilian Agencies: Fundação de Amparo à Pesquisa do Estado de Minas Gerais (FAPEMIG), Conselho Nacional de Desenvolvimento Científico e Tecnológico (CNPq), and FINEP-PRONEX.

[1] A. Ashkin, and J.M. Dziedzic, Science **235**, 1517 (1987).
[2] Axial force: P.A. Maia Neto, and H.M. Nussenzveig, Europhys. Lett. **50**, 702 (2000); Transverse force: P.A. Maia Neto, A. Mazolli, and H.M. Nussenzveig (private communication).
[3] T. Strick, J.F. Alemand, V. Croquette, and D. Bensimon, Prog. Biophys. Mol. Biol. **74**, 115 (2000).
[4] R.M. Simmons, J.T. Finer, S. Chu, and J.A. Spudich, Biophys. J. **70**, 1813 (1996).
[5] M.D. Wang, H. Yin, r. Landick, J. Gelles, and S.M. Block, Biophys. J. **72**, 1335 (1997).
[6] *Photon Correlation and Light Beating Spectroscopy*, edited by H.Z. Cummins and E.R. Pike (Plenum, New York, 1974).

[7] R. Bar-Ziv, A. Meller, T. Tlusty, E. Moses, J. Stavans, and S.A. Safran, Phys. Rev. Lett. **78**, 154 (1997); A. Meller, R. Bar-Ziv, T. Tlusty, E. Moses, J. Stavans, and S.A. Sagran, Biophys. J. **74**, 1541 (1998).
[8] M.C. Wang and G.E. Uhlenbeck, Rev. Mod. Phys. **17**, 323 (1945).
[9] M.I.M. Feitosa and O.N. Mesquita, Phys. Rev. A **44**, 6677 (1991).
[10] L.P. Faucheux and A.J. Libchaber, Phys. Rev. E **49**, 5158 (1994).
[11] L. Lobry and N. Ostrowsky, Phys. Rev. B **53**, 12 050 (1996).
[12] G.V. Shivashankar, G. Stolovitzky, and A.J. Libchaber, Appl. Phys. Lett. **73**, 291 (1998).
[13] J.F. Marko and E.D. Siggia, Macromolecules **28**, 8759 (1995).